Double Star Measures Using the Video Drift Method - II

Richard L. Nugent
International Occultation Timing Association
Houston, Texas
RNugent@wt.net

Ernest W. Iverson
International Occultation Timing Association
Lufkin Texas
ewiverson@consolidated.net

Abstract: This paper gives the position angle and separation for 181 multiple star systems measured using the video drift method from dates September 6, 2010 to July 23, 2011 (2010.767 to 2011.559). The multiple star systems reported on here are located between 2h 03m to 23h 07m Right Ascension and -20° to +50° degrees declination. Preference was given to multiple stars systems with fewer than 35 measurements since their discovery. Factors effecting the position angle and separation standard deviations are discussed. Statistical analysis of results indicates that standard deviations of both position angle and separation are largely due to atmospheric effects and not correlated with variables like star magnitude.

Introduction

In our first paper (Nugent and Iverson, 2011, hereinafter called "Paper I") we described a new method that computes both the position angle (theta or *q*) and the separation (rho or *r*) for a multiple star system using 100's to 1,000's of (*x,y*) positions of the components obtained from a short video clip of the target multiple star system drifting across the field of view. The freeware program *LiMovie* (Miyashita, 2006), originally intended for analysis of occultation data, is used to convert the raw video into a table of (*x,y*) positions for the two component stars being measured. *VidPro*, an Excel program written by co-author RLN, reads the (*x,y*) position data and computes a unique value for the position angle and the separation and other statistical quantities. A detailed description of how to set up and use the *LiMovie* and *VidPro* programs plus a free *VidPro* download link can be found in Nugent (2010). The advantage of using this method is that the data collection and subsequent data analysis is automated and requires little human interaction. The whole recording process can be performed in just a matter of a few minutes per double star system at the telescope with the proper set up. Therefore, this method is ideally suited for survey projects involving hundreds of double stars.

In Paper I we demonstrated the accuracy of this

220 New Wide Common Proper Motion Binaries in the LSPM-North Catalog

Table 1. Telescopes used in this research. Scale factors vary slightly due to the declination of the doubles.

TELESCOPE	APERTURE	FOCAL LENGTH	SCALE FACTOR
Meade LX-200	14" (35cm)	3550 mm f/10	0.6"/pixel
Meade LX-200	8" (20cm)	2000 mm f/10	1.1"/pixel
Questar	3.5" (9cm)	1299 mm f14.4	1.6"/pixel

method by a comparison with double star systems that have shown little or no change in their respective position angles or separations since their discovery. In this paper we focus on the standard deviations for both the position angle and separation computed by the *VidPro* program as a measure for evaluating the quality of each drift.

Method

The multiple star systems reported on here were selected from the Washington Double Star Catalog (WDS). Preference was given to multiple star systems that the WDS reports less than 35 measurements since being discovered. This criterion applies to most, but not all of the multiple star systems measured.

Drift scans made by Nugent used either a Meade 14-inch (35cm) SCT or a 3.5-inch (9cm) Questar telescope equipped with a *Watec 902H2 Ultimate* video camera. The video camera has a built in manual gain adjustment. Almost all of the drift scans made by Iverson used a Meade 14-inch (35cm) LX200 ACF SCT and equipped with either a *Watec 902H2 Ultimate* or a *Stella Cam 3* video camera. Early in the study period, a few drift scans were made using an 8-inch (20cm) Meade LX200 GPS telescope. A *Stella Cam 2* and a *Stella Cam EX* camera were used for a few drifts. All three of the *Stella Cam* cameras (made by Adirondack Video Astronomy) have adjustable gain features and are capable of on camera integration. The integration feature works by combining (stacking) multiple video frames to increase the brightness/visibility of the companion star. This is done automatically by the camera. The user chooses the integration rate before the video is captured.

All measurements made with the Meade telescopes were at f/10 with the exception of WDS 08358+0637 (STF 1245AB). The drift scan of this close double was made with a barlow lens inserted into the light path for better separation of the component stars. Measurements with the Questar were at f/14.4. Scale factors for the equipment were 1.6"/pixel for the Questar, 1.1" /pixel and 0.6"/pixel for the Meade 8"/14"setup respectively. The telescope equipment and scale factors are summarized in Table 1.

The data collection and analysis procedures used follow those described by Nugent (2010) and Paper I. When necessary, the camera gain was adjusted to a point where the dimmest member of the multiple star system would be clearly visible with the *LiMovie* program. The camera's gain setting was also used to reduce over-saturation of target stars with very close separation whenever possible to avoid merging of the components. On camera integration and manual gain adjustment were used by Iverson to enhance dim companion stars to a point where they could be measured by the *LiMovie* program. Both the *Stella Cam 2* (equivalent to the *Watec 120N*) and *Stella Cam 3* used in this study will output the last integrated image while the next image is being formed. A detailed description of the *Watec 120N* camera timing can be found at Dangl (2010).

Using 4 frame integration (0.132 seconds) as an example, these cameras will output a new image in the first frame after the image is formed. The same image is then output for the next 3 successive frames. During frames 1 to 4, the camera is integrating a new image. On the fifth frame, the new image is output. The *Stella Cam EX* (a Mintron camera derivative) conceptually works in the same manner except that it integrates fields instead of frames (Menke 2009). A *Stella Cam EX* camera setting of 4x integrates an image for only 0.066 seconds.

Statistical Results

Figure 1 presents the position angle standard deviation distribution compared to separation. The larger position angle standard deviations are the direct result of closer separations. This is a mathematical consequence and not caused by any optical or real physical effect. This concept is shown in Figure 2.

In Figure 2, diagrams A) and B) each represent a double star system with identical position errors ε indicated by the error bars. The separations are D and D' respectively where D > D'. The quantities ΔPA and ΔPA' *are not* the position angles between the pri-

Double Star Measures Using the Video Drift Method - II

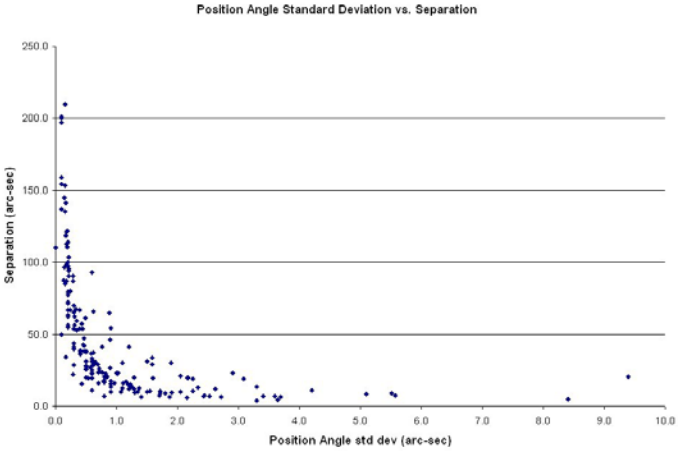

Figure 1. The relationship between the position angle standard deviation and the separations. The larger standard deviations for smaller separations is an expected mathematical result. See text for explanation.

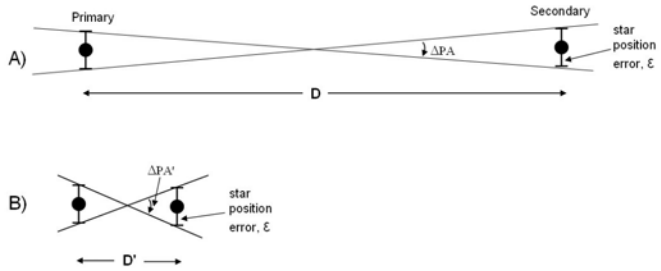

Figure 2. A) and B) are double star systems with separations D and D' where D > D'. The error in star position is denoted by ε. ΔPA and ΔPA' are not the position angles, but rather the error ranges in position angle due to the uncertainty ε of both star positions.

mary and secondary stars. They are the error ranges in position angle PA due to the uncertainty ε in the (x,y) position of *both* stars. For identical ε's , ΔPA' will always be larger than ΔPA. To prove this we derive ΔPA as follows (formulas apply for both diagrams A and B):

$$\tan\left(\frac{1}{2}\Delta PA\right) = \frac{\varepsilon}{\frac{1}{2}D} \qquad (1)$$

or

$$\Delta PA = 2\arctan\left(\frac{\varepsilon}{\frac{1}{2}D}\right) \qquad (2)$$

It follows from equation (2) that if D' < D, then ΔPA' > ΔPA, thus smaller separations lead to larger PA error ranges which equates to larger standard deviations.

Sometimes *LiMovie* has difficulty separating very close pairs (under 5"), depending on star disk sizes plus the degree of atmospheric fluctuation of the seeing disks. A similar plot of the separation standard deviation and the distance between component stars (see Figure 3) does not show as large a range in standard deviation nor any correlation. This shows that the program *LiMovie* has no bias effect in deriving positions of the centroid of each component. Higher standard deviations in this case are probably due to atmospheric effects.

The *LiMovie* 3-D graph in Figure 4 shows distinct light intensity peaks for each star. For close doubles, it is typical to also see a bridge of light energy between the two stars. Even with these light bridges, *LiMovie's* aperture measuring rings and settings can be adjusted to maintain their position directly over the star seeing disks to provide reliable (x,y) data.

Using an integrating camera can be very beneficial in measuring multiple star systems. The obvious benefit is that an integrating camera will extend the magnitude range that can be reached with a given telescope. A second advantage is that it tends to average out variations caused by atmospheric motion. Increasing the integration time made a significant reduction in the standard deviations for the position angle (see Figure 5) and a small decrease in the separation standard deviations. However there are practical limits on the maximum integration time. During long integrations a star appears to move in short jumps on the monitor screen, the length of which is determined by the integration time. With increasing integration times, the star leaves a trailing streak on the monitor screen. With short integration times *LiMovie* can easily track this movement, but has increasing difficulty with successively longer integration times. Even though two successful measurements were made with a *Stella Cam 3* camera at 16 frames of integration, integrations longer than 0.198 seconds (using a *Stella Cam EX)* are impractical. Measurements beyond 4 frames (0.132 sec.) of integration were not attempted on a routine bases with these cameras.

At first we were skeptical that multiple star systems with a large difference in magnitude between the primary star and the companion contributed to

Double Star Measures Using the Video Drift Method - II

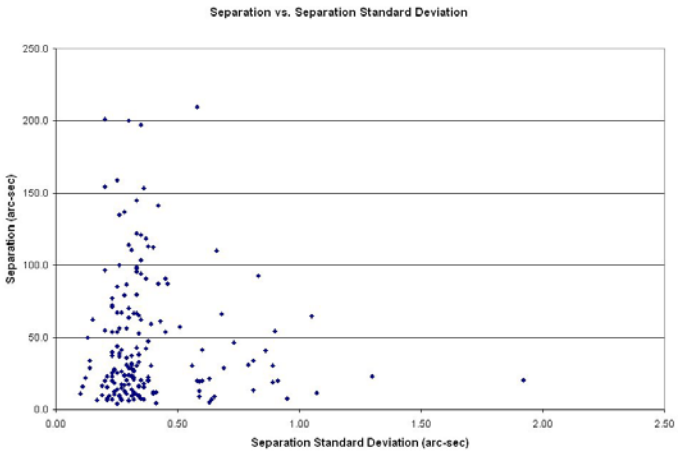

Figure 3. Measured binary star separations in relation to standard deviation.

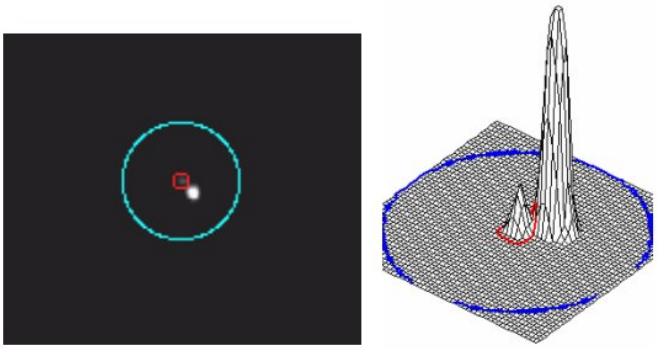

Figure 4: RIGHT: LiMovie 3-D contour plot from a single video frame of the double star system WDS 11551+4629, STF 1579. The contour plot is rotated 45 deg counterclockwise to simplify viewing of the secondary star's aperture ring placement. The measured separation is 3.7 arc-seconds, position angle 42 degrees with standard deviations of 0.17" and 3.8 deg respectively. Notice how the bases of the stars merge together. This shows that LiMovie's aperture controls and constraints can measure even very close doubles. LEFT: Corresponding video frame with North at the top.

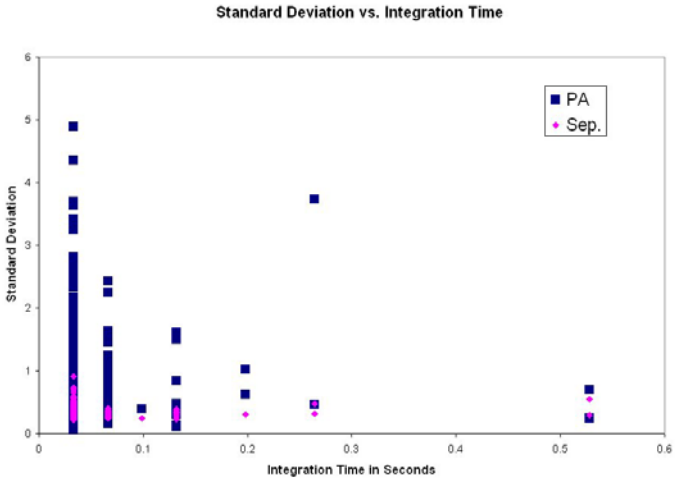

Figure 5. A comparison of the integration times to the PA and Sep standard deviation. As expected, longer integration times help freeze atmospheric motion and reduce standard deviations

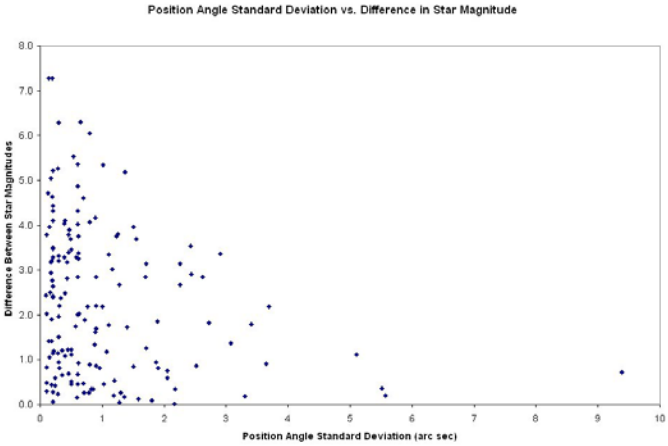

Figure 6. The relationship between the magnitude difference between the primary and secondary star in a double star system and the position angle standard deviation. A large magnitude difference does not contribute significantly to a larger standard deviation.

larger standard deviations. Figures 6 and 7 show that even with the largest magnitude differences, the respective standard deviations did not increase significantly. In fact the largest standard deviations occurred when the stars had similar magnitudes. Figure 8 suggests that bright stars which have a large visual seeing disk do not cause an abnormal increase in the standard deviations. If the *LiMovie* aperture circle is large enough to contain the seeing disk, then the centroiding function will give reliable (*x*,*y*) positions. Measurements with larger standard deviations are probably the result of turbulence in the air column or perhaps high humidity.

Discussion

The statistical results demonstrate that the Earth's constantly fluctuating atmosphere is a signifi-

(Continued on page 221)

Double Star Measures Using the Video Drift Method - II

Table 2. Results for 181 multiple star systems obtained by using the video drift method. The columns are identified as WDS Catalog No., discoverer name, position angle (PA), position angle σ, separation (SEP), separation σ, magnitude of primary and secondary (taken from WDS Catalog), no. of (*x*,*y*) pairs in the drift, date and no. of independent drifts.

WDS	Discoverer	PA°	σ-PA	Sep"	σ-SD	mag Pri	mag Sec	No. (x,y) Pairs[1]	Date	No. Drifts[2]
02305+0314	BAL1624	235	8.4	4.9	0.6	9.8	10.2	606	2010.899	
02430-2017	HJ 3524	166	1.6	19.7	0.6	7.67	9.16	741	2010.896	
03187-1834	HJ 3565	124	3.6	6.9	0.6	5.88	8.17	727	2010.896	
03505-1219	GAL 357	148	1.2	41.0	0.9	9.28	11.3	714	2011.003	
04311+0647	STT 84	256	1.9	9.7	0.3	7.23	8.11	720	2011.092	
05353-0523	STF 748CD	62	3.3	13.4	0.8	5.06	6.38	1838	2011.077	
05387-0236	STF 762AB,E	61	0.8	41.4	0.6	3.76	6.34	1242	2011.137	
05387-0236	STF 762ED	232	1.1	30.2	0.6	6.34	6.56	1211	2011.137	
05387-0236	STF 762AB,D	84	2.3	12.9	0.6	3.76	6.56	1266	2011.137	
05387-0236	STF 762AF	324	0.2	209.6	0.6	3.76	7.86	998	2011.137	
06389+2748	STT 151AB	131	1.6	29.1	0.7	7.35	10.40	1379	2011.121	
06439+2508	S 533	95	0.0	110.1	0.7	3.14	9.64	1147	2011.121	
06555+3755	STF 978AB	82	2.2	19.8	0.6	6.85	10.00	1559	2011.121	
07058-1040	STF1019AC	292	0.5	38.2	0.3	6.51	9.55	1326	2011.208	2
07067-1118	STF1026AB-C	350	0.9	17.8	0.4	5.39	9.0	1432	2011.208	2
07321-0853	STF1112	114	0.7	23.8	0.3	6.03	8.73	1320	2011.208	2
07328+2253	STF1108	177	4.2	11.24	1.1	6.0	6.73	2176	2011.230	
07455-1441	STF1138AB	339	0.8	16.8	0.3	6.0	6.73	1446	2011.208	2
07583+0213	SHJ 87AC	149	0.1	136.9	0.3	5.41	9.89	527	2011.195	
07583+0213	SHJ 87AB	84	0.2	100.2	0.3	5.41	9.36	527	2011.195	
08065-0915	STF1183AB	328	0.5	31.0	0.3	6.22	7.77	1398	2011.208	2
08113-1256	SHJ 91AE	256	0.3	70.1	0.3	4.82	9.37	1222	2011.208	2
08113-1256	ARY 64AF[3]	329	0.2	114.1	0.3	4.82	-	1208	2011.208	2
08158+0248	STF1210AB	115	0.9	15.6	0.2	7.25	9.45	1388	2011.195	2
08285-0231	STF1233AB-C	330	0.8	18.3	0.2	6.42	10.49	2067	2011.195	3
08358+0637	STF1245AB[4]	25	1.1	10.3	0.2	5.98	7.16	533	2011.137	
08397+0546	STF1255AB	30	0.5	26.3	0.3	7.33	8.56	2073	2011.205	3
08399+1933	S 571AD	242	0.6	92.87	0.8	7.31	7.47	1871	2011.230	
08437-0714	S 579AB	310	0.2	79.3	0.3	4.72	8.2	1180	2011.208	2
08467+2846	STF1268	308	1.9	30.38	0.9	4.13	5.99	2194	2011.230	
08516-0711	H 5 120AB-C	5	0.9	46.3	0.7	5.54	9.7	673	2011.205	
08552-1814	S 585	151	0.9	64.77	1.1	5.9	7.24	2028	2011.230	
08553-1122	S 584	217	0.3	65.2	0.3	6.88	8.84	1326	2011.208	2
09003+0332	HJ 2479	323	2.9	23.1	1.3	8.99	12.35	694	2011.107	
09008-0911	BU 409	187	0.9	10.2	0.2	7.25	10.1	2162	2011.205	4
09074+2259	STF1311AB	199	5.6	7.41	1.0	6.92	7.13	1907	2011.342	
09091-0135	HJ 119	331	0.9	54.4	0.9	7.8	9.5	678	2011.107	
09144+0219	HJ 2489AB	243	0.8	20.4	0.3	3.85	9.9	2037	2011.195	3
09175+0033	STF1336	181	0.3	41.2	0.3	7.0	10.2	2104	2011.205	3
09205-0933	DOO 49BC	199	1.5	9.9	0.3	7.03	10.99	2130	2011.205	3
09283-0959	STF1357	54	2.4	7.6	0.4	6.94	9.85	733	2011.205	
09285+0811	H4 47	80	0.6	25.2	0.3	5.76	11.12	1336	2011.195	2

Table 2 continues on next page.

Double Star Measures Using the Video Drift Method - II

Table 2 (continued). Results for 181 multiple star systems obtained by using the video drift method. The columns are identified as WDS Catalog No., discoverer name, position angle (PA), position angle σ, separation (SEP), separation σ, magnitude of primary and secondary (taken from WDS Catalog), no. of (*x*,*y*) pairs in the drift, date and no. of independent drifts.

WDS	Discoverer	PA°	σ-PA	Sep"	σ-SD	mag Pri	mag Sec	No. (x,y) Pairs[1]	Date	No. Drifts[2]
09291-0246	HJ 1167	4	0.2	67.1	0.3	4.64	7.28	3230	2011.205	3
09307+3339	HJ 1166AB	125	0.5	61.3	0.4	5.97	9.66	1433	2011.121	
09320+0943	SHJ 107	75	0.4	37.5	0.2	5.2	9.3	1947	2011.195	3
09412+0954	H6 76AB	47	0.1	96.8	0.2	3.56	10.83	1048	2011.233	2
09541+0457	S 605	287	0.3	53.7	0.2	6.89	8.4	1873	2011.195	3
09587+1058	H5 63AB	348	0.1	49.7	0.1	7.47	9.5	2127	2011.195	3
10040-1806	HJ 110	274	2.1	21.2	0.6	6.22	6.97	1908	2011.279	
10097+0310	STF1412AC	52	0.3	90.6	0.5	8.49	8.72	537	2011.203	
10125+0245	BAL2370	57	9.4	20.4	1.9	6.0	6.73	576	2011.203	
10129+0221	BAL1870	10	3.1	19.0	0.9	10.23	11.6	648	2011.203	
10220+4354	STF1427	215	5.5	9.18	0.7	8.18	8.54	2611	2011.340	
10223+0317	SLE 585	9	1.6	33.7	0.8	11.17	11.29	677	2011.203	
10237+0237	BUP 132AC	138	0.1	154.6	0.2	7.94	11.73	533	2011.340	
10242+0222	HJ 2530AC	64	0.1	201.0	0.2	6.42	6.72	1035	2011.342	3
10344+2136	STF1448AC	259	0.6	10.9	0.1	7.54	9.55	4533	2011.233	6
10433+0445	STF1466AB	239	0.8	6.9	0.2	6.23	7.13	699	2011.205	
10459_3041	S 612AB	174	0.1	200.3	0.3	5.34	7.78	800	2011.326	
10476-1516	STF1474AB	27	0.6	66.03	0.7	6.67	7.59	1879	2011.340	
10534-0215	S 617	179	0.4	36.1	0.3	6.22	8.71	2112	2011.205	3
10556+2445	STF1487	114	2.7	6.6	0.3	4.48	6 .30	785	2011.326	
11118+4250	ENG 45AB	247	0.2	135.2	0.3	7.24	8.30	661	2011.329	
11125+3549	STTA108AB	68	0.1	159.0	0.3	6.48	7.32	2451	2011.326	2
11167-0339	SHJ 121	291	0.3	87.2	0.5	4.48	9.75	553	2011.340	
11194-0139	STF1529	254	1.9	9.4	0.3	7.10	7.91	2561	2011.340	2
11256+1627	HJ 4433AB	3	0.2	56.2	0.3	5.62	10.84	1469	2011.263	2
11268+0301	STF1540AB	150	0.3	28.7	0.1	6.55	7.50	2640	2011.340	2
11279+0251	STFA 19AB	181	0.2	90.7	0.4	5.05	7.47	699	2011.348	
11317+1422	STF1547AB	331	0.4	15.7	0.1	6.33	9.14	2939	2011.233	4
11347+1648	STF1552AC	235	0.2	63.5	0.3	6.26	9.77	652	2011.263	
11363+2747	HJ 503AB,C	158	1.0	22.5	0.4	5.83	11.17	812	2011.279	
11396+1900	STF1565	305	0.3	21.9	0.1	7.26	8.41	3771	2011.233	5
11480+2013	STF B 7AB	356	0.2	77.4	0.2	4.59	9.03	744	2011.263	
11520+0850	STF1575	210	0.6	31.0	0.3	7.43	7.89	2700	2011.263	2
11528+1526	SHJ 132AB	14	0.3	39.7	0.2	6.86	10.17	1460	2011.263	2
11551+4629	STF1579AB,D	114	0.2	62.2	0.2	6.68	6.97	3412	2011.279	2
12095-1151	STF1604AC	14	1.7	10.5	0.3	6.86	8.12	760	2011.414	
12095-1151	STF1604AB	88	1.7	9.1	0.3	6.86	10.00	731	2011.414	
12141+3247	STF1615AB	87	0.9	26.8	0.3	6.99	8.61	788	2011.323	
12145+0847	STF1616AB	296	0.8	23.4	0.3	7.55	9.74	702	2011.263	
12161+4040	STF1622	257	2.6	11.9	0.4	5.86	8.71	921	2011.323	
12182-0357	STF1627	196	0.8	20.2	0.4	6.55	6.9	2055	2011.342	2
12202+3754	STF1632	193	2.3	10.8	0.4	6.83	9.98	901	2011.323	

Table 2 continues on next page.

Double Star Measures Using the Video Drift Method - II

Table 2 (continued). Results for 181 multiple star systems obtained by using the video drift method. The columns are identified as WDS Catalog No., discoverer name, position angle (PA), position angle σ, separation (SEP), separation σ, magnitude of primary and secondary (taken from WDS Catalog), no. of (*x*,*y*) pairs in the drift, date and no. of independent drifts.

WDS	Discoverer	PA°	σ-PA	Sep"	σ-SD	mag Pri	mag Sec	No. (x,y) Pairs[1]	Date	No. Drifts[2]
12207+2703	STF1633	245	1.8	9.0	0.3	7.04	7.13	2440	2011.323	2
12225+2551	SHJ 143AC	168	0.4	66.8	0.3	4.86	8.90	773	2011.323	
12281+4448	STF1645	157	2.1	9.9	0.3	7.49	8.08	1010	2011.323	
12289+2555	STFA 21AB	250	0.1	144.8	0.3	5.23	6.64	492	2011.323	
12351+1823	STF1657	270	0.5	20.0	0.2	5.11	6.33	2796	2011.326	2
12387-0422	S 639AB	110	0.4	57.1	0.5	6.82	9.99	280	2011.340	
12453-0353	STF1677	349	1.0	16.3	0.3	7.30	8.12	721	2011.340	
12454+1422	STF1678	171	0.5	37.7	0.3	7.16	7.68	2630	2011.348	2
12519+1910	STF1685AB	201	0.7	16.3	0.2	7.31	7.78	2681	2011.326	2
12522+1704	STF 23AB	51	0.1	197.0	0.4	6.50	6.99	422	2011.348	
12533+2115	STF1687AC	128	0.7	29.1	0.3	5.15	9.76	726	2011.326	
12555+1130	STF1689	222	0.6	30.3	0.3	7.11	9.13	694	2011.340	
12560+3819	STF1692	228	2.3	19.3	0.6	2.85	5.52	4826	2011.334	2
13062+4055	HJ 2639AC	138	0.4	53.6	0.3	7.48	10.77	888	2011.323	
13062+4055	HJ 2639BC	102	1.0	23.2	0.3	11.23	10.77	846	2011.323	
13062+4055	HJ 2639AB	159	0.6	37.2	0.3	7.48	11.23	848	2011.323	
13169+1701	BU 800AB	108	1.7	7.5	0.2	6.66	9.50	1506	2011.326	2
13237+0243	STF1740	74	0.7	26.3	0.3	7.13	7.39	691	2011.340	
13282+0928	STF1746	245	1.0	23.1	0.3	7.61	9.80	1070	2011.326	2
13356+1012	HJ 228	15	0.2	71.3	0.2	6.60	8.99	1373	2011.326	2
13377+0223	STF1764AB	31	1.1	16.0	0.3	6.79	8.56	720	2011.340	
13435-0416	STF1775AB	335	0.6	28.2	0.3	7.21	10.06	699	2011.414	
13470+3833	S 654AB	236	0.2	72.4	0.2	5.62	8.91	1556	2011.323	2
13504+2117	S 656	208	0.2	86.9	0.3	6.93	7.37	671	2011.326	
13547+1824	SHJ 169	86	0.2	113.1	0.4	2.72	9.99	516	2011.425	
14048+2549	BGH 50	32	0.2	98.8	0.3	7.00	8.90	661	2011.416	
14067+3447	STT 274	52	1.1	12.5	0.2	7.13	10.47	1703	2011.323	2
14226-0746	STF1833AB	175	2.2	6.0	0.3	7.51	7.52	719	2011.414	
14234+0827	STF1835A,BC	194	1.4	6.4	0.2	5.03	6.76	2900	2011.419	4
14241+1115	STF1838	335	1.3	9.5	0.2	7.47	7.73	1446	2011.419	2
14253-1321	HJ 546	46	0.5	42.5	0.4	6.60	10.00	673	2011.414	
14286+2817	STF1850	261	0.5	25.5	0.2	7.11	7.56	1524	2011.416	2
14407+1625	STF1864AB	114	3.6	4.3	0.4	4.88	5.79	753	2011.425	
14514+1906	STF1888AB	301	3.7	6.7	0.3	4.76	6.95	748	2011.425	
14576-0010	H 6 51AB	223	0.1	87.3	0.4	5.64	10.36	1837	2011.367	3
14589-1109	STF1894AB	38	0.6	19.7	0.2	5.87	9.90	1472	2011.367	2
15006+4717	STT 291	157	0.6	36.8	0.3	6.33	9.62	1042	2011.436	
15016-0310	STF1899	67	0.5	28.0	0.2	6.69	10.15	1350	2011.414	2
15041+0530	STF1904	348	1.4	10.3	0.3	7.19	7.37	745	2011.367	
15075+0914	STF1910	210	3.3	4.0	0.3	7.35	7.54	1392	2011.367	2
15127+1917	STF1919	10	0.6	22.9	0.2	6.71	7.38	1508	2011.416	2
15141+3147	STT 292	158	0.2	121.2	0.4	6.16	9.36	741	2011.416	

Table 2 continues on next page.

Double Star Measures Using the Video Drift Method - II

Table 2 (continued). Results for 181 multiple star systems obtained by using the video drift method. The columns are identified as WDS Catalog No., discoverer name, position angle (PA), position angle σ, separation (SEP), separation σ, magnitude of primary and secondary (taken from WDS Catalog), no. of (*x*,*y*) pairs in the drift, date and no. of independent drifts.

WDS	Discoverer	PA°	σ-PA	Sep"	σ-SD	mag Pri	mag Sec	No. (x,y) Pairs[1]	Date	No. Drifts[2]
15155+3319	STFA 27	79	0.2	103.5	0.4	3.56	7.89	604	2011.416	
15158+5056	STTA137	102	0.3	67.3	0.3	6.56	8.94	958	2011.436	
15187+1026	STF1931AB	167	0.9	13.7	0.3	7.20	8.07	1432	2011.367	2
15245+3723	STF 28AB	171	0.2	110.6	0.3	4.33	7.09	860	2011.416	
15282-0921	SHJ 202AB	133	0.4	52.8	0.3	6.95	7.61	648	2011.367	
15382+3615	STF1964AC	84	1.2	15.1	0.3	7.85	8.06	878	2011.416	
15387-0847	STF1962	189	1.3	12.0	0.3	6.44	6.49	764	2011.367	
15394+3638	STF1965	307	1.9	6.4	0.2	4.96	5.91	1725	2011.416	2
15402+1203	STT 300	260	1.2	15.3	0.4	6.32	10.07	702	2011.419	
15462+1525	STF1970AB	264	0.7	30.6	0.4	3.66	9.96	696	2011.425	
15549+3422	STT 302AB	50	0.6	28.7	0.3	7.16	10.42	817	2011.416	
16010+3318	S 676	46	0.2	141.4	0.4	5.47	10.51	611	2011.416	
16044-1127	STF1999AB	99	1.2	11.9	0.4	7.52	8.05	1249	2011.367	2
16060+1319	STF2007AB	323	0.4	38.9	0.3	6.89	7.98	1385	2011.419	2
16081+1703	STF2010AB	13	0.5	27.6	0.2	5.10	6.21	1498	2011.419	2
16118+4222	STF2024	44	0.6	22.8	0.2	5.86	10.73	1865	2011.416	2
16147+3352	STF2032AB	237	2.5	7.1	0.3	5.62	6.49	875	2011.416	
16201-2003	SHJ 225	334	0.5	47.4	0.4	7.39	8.08	763	2011.367	
16212-2536	H 4 121AB	271	0.5	19.8	0.4	2.89	8.42	2306	2011.367	3
16219+1909	SHJ 227AB	226	0.3	43.9	0.3	3.76	10.05	1400	2011.419	2
16229+3220	H5 38	16	0.6	31.7	0.3	6.41	9.79	828	2011.416	
16315+0818	SHJ 233	70	0.4	59.4	0.4	7.07	8.28	609	2011.419	
16318+4536	STF2063	196	1.2	17.2	0.3	5.69	8.70	1036	2011.436	
16424+2136	STF2085	306	3.4	6.9	0.3	7.38	9.17	761	2011.425	
16435+2043	STTA149	135	0.2	97.7	0.3	7.24	8.38	643	2011.425	
16436+0637	H5 127	294	0.4	53.8	0.5	7.81	9.04	627	2011.419	
16458+0835	SHJ 239AB	228	0.2	85.2	0.3	5.33	9.29	1760	2011.419	3
17048+2805	STF2120AB	230	0.7	24.0	0.3	7.37	9.25	782	2011.425	
17150+2450	STF3127AB	285	1.4	12.8	0.3	3.12	8.30	784	2011.425	
17391+0202	SHJ 251AB	329	0.2	112.7	0.4	6.37	7.78	597	2011.482	
17446+0235	STF2202AB	93	0.8	20.7	0.3	6.13	6.47	683	2011.482	
17521+0107	S 694	238	0.2	79.9	0.3	6.67	7.26	581	2011.482	
18002+0851	STTA161AB	72	0.3	62.5	0.4	6.99	9.19	619	2011.482	
18006+0256	H6 2AC	143	0.2	54.9	0.2	3.96	8.06	1912	2011.482	3
18078+1304	H5 74	140	0.5	42.6	0.3	6.60	10.39	669	2011.482	
18334+0816	STT 355	248	0.5	38.1	0.3	6.41	10.31	651	2011.482	
18356+0456	STF2342AC	359	0.2	34.1	0.1	6.46	9.63	726	2011.482	
18545+0154	STTA176AB	293	0.2	94.3	0.4	7.45	7.51	560	2011.482	
18562+0412	STF2417AB	104	0.8	22.5	0.3	4.59	4.93	675	2011.482	
19302+0254	STF2532AB	2	0.6	33.0	0.3	6.27	10.60	709	2011.559	
19302+0254	STF2532AC	196	0.2	121.8	0.3	6.27	10.91	652	2011.559	
19302+0254	STF2532BC	193	0.2	153.6	0.4	10.60	13.10	652	2011.559	
19362+0600	STF2543	151	1.6	10.8	0.3	6.76	10.45	727	2011.559	

Table 2 concludes on next page.

Double Star Measures Using the Video Drift Method - II

Table 2 (conclusion). Results for 181 multiple star systems obtained by using the video drift method. The columns are identified as WDS Catalog No., discoverer name, position angle (PA), position angle σ, separation (SEP), separation σ, magnitude of primary and secondary (taken from WDS Catalog), no. of (*x*,*y*) pairs in the drift, date and no. of independent drifts.

WDS	Discoverer	PA°	σ-PA	Sep"	σ-SD	mag Pri	mag Sec	No. (x,y) Pairs[1]	Date	No. Drifts[2]
19428+0823	STF2562AB	251	0.6	27.3	0.3	6.95	8.69	709	2011.559	
19428+0823	STF 256AD	221	0.2	118.5	0.4	6.95	9.89	605	2011.559	
19428+0823	STF 256BD	213	0.2	95.7	0.3	8.69	9.89	628	2011.559	
19523+1021	STF2590AB	308	1.3	13.7	0.3	6.50	10.31	730	2011.559	
20066+0735	STTA198AB	186	0.2	66.7	0.3	7.12	7.55	715	2011.559	
20101+0827	STF2635AB	79	2.4	7.1	0.4	6.66	10.19	697	2011.559	
20113-0008	S 735	210	0.3	56.1	0.3	7.16	7.98	664	2011.559	
20312+1116	STF2690A,BC	255	0.8	17.6	0.3	7.12	7.39	717	2011.559	
21069+3845	STF2758AB	152	1.5	31.1	0.8	5.2	6.05	2242	2010.767	
23075+3250	STF2978	142	5.1	8.8	0.6	6.35	7.46	2170	2010.767	

Table 2 Notes:

1. For multiple drifts (*x*,*y*) pairs are the sum total from all drifts combined
2. For multiple drifts, PA, SEP and σ's are weighted means
3. WDS 08113-1256, ARY 64AF, No companion star magnitude was available from WDS
4. WDS 08358+0637, STF 1245AB, Barlow lens used

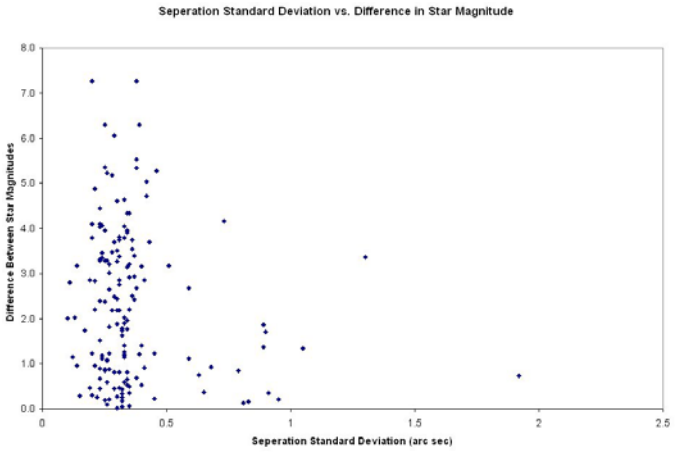

Figure 7. The relationship between the magnitude difference of the primary and secondary star in a double star system and the separation standard deviation.

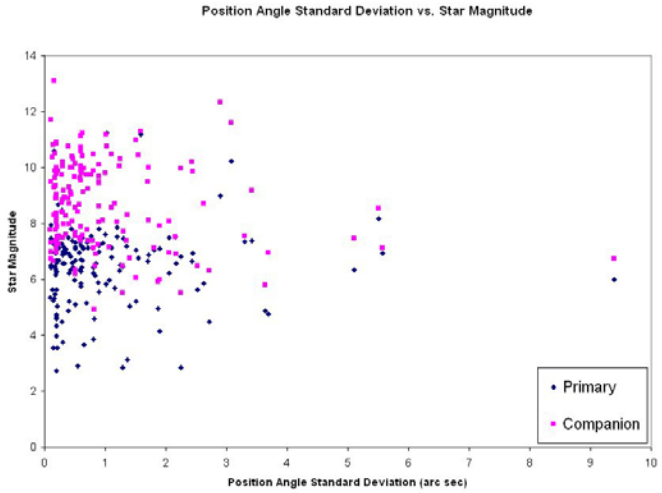

Figure 8. The WDS star magnitudes in relation to the position angle standard deviation. In general bright stars do not significantly result in higher standard deviations. Higher standard deviations are most likely due to atmospheric conditions.

(Continued from page 216)

cant contribution to the observed standard deviations (σ's) using this video drift method. Our method picks up atmospheric fluctuations every 0.033 sec defined by the NTSC video standard used by our video cameras. Thus our σ's are a measure of the steadiness of the atmosphere during the 30-60 second videos. The video drift method accumulates 30 (*x*,*y*) measurements each second for each star. Every 0.033 second a new PA and separation is computed based on incremental changes of their (*x*,*y*) positions due to atmospheric fluctuations and the drift. The final PA and separation are averages of all values for all frames during the drift. An unsteady atmosphere will cause more fluctuations, while a steady atmosphere will have less fluctuations and hence smaller σ's.

Compare this to a 3-second CCD exposure. Here, the resultant image is the sum total of all seeing disk motion caused by the atmospheric fluctuations during these 3 seconds. The σ's would be dependant on the algorithm used for determining the centroid of the central pixel of this single star image. For multiple CCD images that are averaged, the σ's for PA and SEP would be proportional to where N is the number of CCD images exposed and $\sqrt{1/N}$ measured.

On the surface, the CCD method might appear to be more accurate with its lower standard deviations. In reality, the CCD images have hidden the atmospheric motions that the video drift method has identified and measured. With the large unprecedented number of data points generated by our video method, it provides consistently good results and we believe higher systematic accuracy.

To minimize the effects of the atmosphere, we observe on nights of steady seeing and choose doubles that are on or within 1 hour of the meridian to minimize the air mass the starlight travels through.

Acknowledgements

This research has made use of the Washington Double Star Catalog maintained by the U.S. Naval Observatory.

References

Dangl, G. 2010, *Measurements of Exposure and Internal Delay on Video Cameras for use with Video Time Inserter*, http://www.dangl.at/ausruest/vid_tim/vid_tim1.htm

Menke, J. 2009, *The Timing Logic of the Mintron Integrating Video Camera*, http://menkescientific.com/mintron-timing.pdf

Miyashita, K. 2006, *LiMovie, Light Measurement Tool for Occultation Observation Using Video Recorder,* http://www005.upp.so-net.ne.jp/k_miyash/occ02/limovie_en.html

Nugent, R. 2010, *A New Video Method to Measure Double Stars,* http://www.poyntsource.com/Richard/double_stars_video.htm

Nugent, R. and Iverson, E. 2011, *Journal of Double Star Observations*, 7*,* No. 3, 185-194 (Paper I)

Richard Nugent holds BS, MS degrees in astronomy from the University of South Florida, and since 1998 is the Executive Secretary of the International Occultation Timing Association.

Ernest Iverson is a retired aerospace engineer and avid amateur astronomer. He has been interested in double stars for over 15 years.